

Article

High-Resolution Interannual Evolution of the Dune Toe at a Mesotidal Barrier (Camposoto Beach, SW Spain)

Cristina Montes ¹, Javier Benavente ², María Puig ³, Juan Montes ², Lara Talavera ⁴
and Theocharis A. Plomaritis ^{1,*}

¹ Department of Applied Physics, Faculty of Marine and Environmental Sciences, Marine Research University Insitute (INMAR), University of Cádiz, 11510 Puerto Real, Cádiz, Spain; cristina.montes@uca.es

² Department of Earth Sciences, Faculty of Marine and Environmental Sciences, Marine Research University Insitute (INMAR), University of Cádiz, 11510 Puerto Real, Cádiz, Spain; javier.benavente@uca.es (J.B.); juan.montes@uca.es (J.M.)

³ TECNALIA, Basque Research and Technology Alliance (BRTA), Astondo Bidea, Edificio 700, 48160 Derio, Bizkaia, Spain; maria.puig@tecnalia.com

⁴ Department of Biology, Geology, Physics and Inorganic Chemistry, ESCET, Rey Juan Carlos University, Tulipán St., 28933 Móstoles, Madrid, Spain; lara.talavera@urjc.es

* Correspondence: haris.plomaritis@uca.es

Abstract: Over recent years, processes related to marine storms, sediment shortages and human intervention have caused the global retreat of many coastal systems and the degradation of their dunes. In this context, changes in the dune toe are commonly used as a proxy to study the interannual shoreline evolution, and it is usually analyzed using orthophotography, while high temporal- and spatial-scale resolution studies of dune toe evolution are not frequent. In this work, a quasi-monthly study of dune toe data was carried out between 2008 and 2018. These data, taken from the RTK-DGPS and UAS systems, were subjected to shoreline analysis, and they showed an average regression rate of -2.30 m/year, a higher value than the one registered until 2008 (1 m/year). This suggests an acceleration in the erosion suffered within the system, which was revealed to be more intense in the northern sector of the study area. Dune toe variability increased over the years, probably due to the presence of washover fans breaking the foredune that were reactivated and expanded during storm events. The ephemeral progradation of the dune toe was also noted, which could be explained with reference to wind events and/or beach nourishment that had been carried out over the studied period. From the analysis of the dune toe elevation, a decrease in this variable was obtained, especially in the areas affected due to washover fans. This finding is supported by the significant correlation of the dune toe elevation and erosion trend, suggesting that the areas where the dune toe was lower are prone to suffering a greater retreat. This correlation provides insight into the future evolution of the barrier, suggesting a state of degradation and a transition to a lower-resilience state.

Keywords: dune toe dynamics; coastal retreat; barrier dynamics



Citation: Montes, C.; Benavente, J.; Puig, M.; Montes, J.; Talavera, L.; Plomaritis, T.A. The High-Resolution Interannual Evolution of the Dune Toe at a Mesotidal Barrier (Camposoto Beach, SW Spain). *J. Mar. Sci. Eng.* **2023**, *12*, 718. <https://doi.org/10.3390/jmse12050718>

Academic Editor: Felice D'Alessandro

Received: 6 March 2024

Revised: 18 April 2024

Accepted: 22 April 2024

Published: 26 April 2024



Copyright: © 2023 by the authors. Licensee MDPI, Basel, Switzerland. This article is an open access article distributed under the terms and conditions of the Creative Commons Attribution (CC BY) license (<https://creativecommons.org/licenses/by/4.0/>).

1. Introduction

Barrier islands and spits are dynamic sedimentary features that occupy 6.5% (15,000 km) of the world's sandy open shorelines [1]. Their formation, stability and evolution are the results of a complex interaction between internal and external forcing parameters, such as marine processes (e.g., waves, tides, currents, storminess and relative sea levels), the available sediment budget [2], and aeolian [3] and biological processes [4], acting at various spatiotemporal scales [5,6]. When this continuous interaction between processes leads to barriers' migration, additional environmental parameters like the antecedent geology [7] and anthropic agents that determine the accommodation space can also be important.

Overwash processes during a storm tend to remove sediment from the beach dunes and deposit it in the back barrier area [8,9]. This is a short-scale process that is aggregated

over time, and it can lead to foreshore erosion, beach width reduction, dune fragmentation and eventually barrier migration. Barrier migration rates have often been observed to be discontinuous (punctuated), even alongside steady sea level rise rates. The main mechanism behind this behavior has been suggested to be internal barrier dynamics related to time lags in the shoreface response to barrier overwash [10] or dune dynamics when the storm return period and the characteristic time scale of dune growth are of similar magnitudes [11].

Internal barrier dynamics arise from the interrelated geomorphological units (and associated habitats) present. The primary subaerial area can be divided into units dominated by wave, wind and tidal processes, representing beaches, dunes and marshes [12]. Sandy beaches, considered sediment sources (or sinks) whose widths and slopes are controlled via marine processes, are associated with the landward transport of sand under optimal wind conditions, which is a key aspect of dune construction [13–15]. Dune systems are one of the most interesting habitats, given their role in the evolution of barrier islands. In this sense, the evolution of the foredune is controlled via wind action and interactions with a complex ecosystem, which are influenced and conditioned by numerous factors [16,17]. Finally, the sheltered back-barrier area is usually comprised of lagoons, tidal flats and marshes that separate the barrier itself from the mainland [18,19]. The presence and dimensions of these three units have been used to estimate the state resilience pathways of barrier islands over time [12,20]. The presence of beach–dune systems implies increased resilience, given the existence of a natural defense mechanism against extreme events, since their dynamism allows the cushioning and dissipation of energy, avoiding or delaying the incursion of water inland, as well as the general erosion of the environment and the permanent sediment loss that it entails [21,22]. Despite this interdependence of beach–dune systems, they have traditionally been managed separately with an almost exclusive focus on ecological or touristic values, considerably limiting their functions and future resilience [23,24].

A fundamental step towards the identification of the morphological units described is the determination of usable proxies to clearly distinguish each of them. The dune toe (or dune foot) is the boundary of the beach–dune interface, and it can be defined as the most seaward extension of aeolian processes and deposits [25]. A dune toe can be eroded due to extreme or modal marine storm events. As Smith et al. [25] summarized, the dune toe has been frequently used as a proxy for storm impacts, shoreline retreat, dune erosion, beach–dune processes interpretation and dune recovery. Normally, the identification of a dune toe is determined by means of photointerpretation or, less commonly, via direct field identification.

The dune toe position (horizontal and vertical) has been used in many studies to identify whether the system is in retreat, in equilibrium or in progradation [26–33]. The aim of this work is to analyze the behavior of a beach–dune system situated in a central part of a barrier system (Camposoto, San Fernando, SW Spain) for a 10-year period (2008–2018) using field-based, high-resolution dune toe data as a proxy instead of traditional orthophotography-based regional studies. This approach serves to quantify the trend of the system and compare it with regional-scale estimations, constituting a first step in the analysis of the evolution of the Sancti Petri barrier system.

2. Study Area

Camposoto Beach is located on the southwest (Atlantic) coast of the Iberian Peninsula in the province of Cadiz. The area is part of the northern section of the Sancti Petri sand spit (San Fernando municipality) (Figure 1) extended along 5 km in a NNW–SSE direction as a consequence of the littoral drift that flows in a SE direction [23,34].

Camposoto is a sandy beach backed by a low dune ridge with an average height between 4 and 6 m; it is sparsely vegetated and interrupted by various washover fans, which is part of Natural Park Bahía de Cádiz due to its ecosystemic diversity and landscapes [34,35]. According to the Habitats Directive (Council Directive 92/43/EEC), the Camposoto dunes are included in the dune system of ‘El Chato-Sancti Petri’, which includes several Habitats

of Community Interest, such as embryonic shifting dunes (HCI 2110), shifting dunes along the shoreline—‘white dunes’ (HCI 2120)—and humid dune slacks (HCI 2190). The Camposoto dunes have also been classified as vulnerable due to both the geomorphological condition of the system and its marine influence, following the Dune Vulnerability System (DVS) developed by García-Mora et al. [16] for dunes located in the SW of the Iberian Peninsula. The beach is backed by a wide salt marsh area. The salt marsh is prolonged seawards as a peat outcrop (fossil salt marsh) buried under the present dune–beach area, and it is occasionally exposed after high-energy events at low intertidal levels.

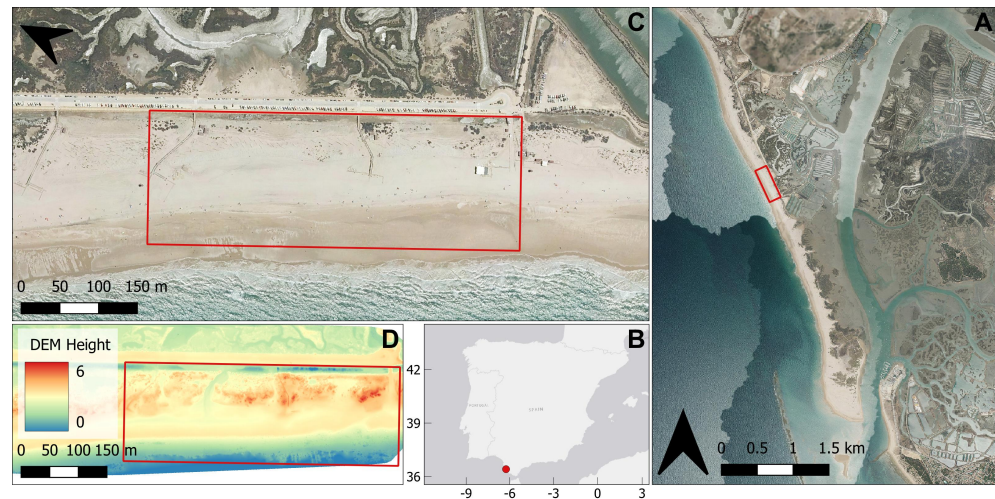


Figure 1. Aerial photograph of the Sancti Petri barrier system (A) located in the southwest of Spain (B). Detail of the study area (the southern section of Camposoto Beach (C)) is presented together with a DTM (Digital Terrain Model) of the beach–dune system (D). Source: National Plan of Aerial Orthophotography (PNOA, 2019).

The study area can be characterized as a wave-dominated and low-energy beach (about 70% of the incident waves register significant heights below 1 m) composed of medium quartz sands, and it presents a profile that exhibits seasonal changes between intermediate and dissipative levels related to low- and high-energy periods [36,37]. The tides are semidiurnal and mesotidal, with a spring tidal range of 3.12 m [38]. The greatest storm events mainly occur between November and March, and they approach the coast from a W–SW direction [39]. The number and magnitude of these storms are affected by atmospheric circulation, more specifically the North Atlantic Oscillation (NAO); when the NAO index is negative, a greater number of storms occur in the Gulf of Cadiz [40,41].

Although there is a bimodal wind regime in the area (Figure 2A), only the westerly winds have enough fetch to generate swell-type waves (Figure 2B). On the other hand, even though the easterly winds are more intense and, thus, favorable for dune formation (low moisture content and high speeds), their generating capacity is limited, as they blow almost parallel to the coast. Accordingly, the Camposoto dunes, as well as most of the dunes in the littoral of Cadiz, are formed via westerly winds, which blow perpendicularly and/or obliquely to the coast (Figure 2B; [42]).

A rollover process has been identified for the Sancti Petri spit with retreat rates of around 1 m per year [35,43–45]. As a result, the migration of the sand spit has occurred landwards as sea storms have activated the overwash processes and deposited the eroded material behind the dunes [34,39]. Evidence of this rollover process that has been recorded during the last decade encompasses the recession of the dune toe quantified by del Río et al. [29] between 1956 and 2008, the fragmentation of the foredune ridge and the outcropping of ancient salt marsh depositions observed by Talavera et al. [46] in the intertidal zone of the beach after storm events.

Between the beach–dune system and the back barrier area, there are several anthropic elements, such as accesses and wooden walkways placed on the dunes, parking lots, a road,

an artificial channel and an adjoining promenade built in recent years that shows stability problems (Figure 1). This infrastructure is permanent, and it contributes to the debilitation of the dune ridge and the interruption of the onshore sediment transport during overwash. As a consequence, the dunes' landward migration and the system's rollover are restrained. In addition, various removable infrastructure elements are installed during the summer season at the upper part of the beach to serve visitors. This generates significant anthropic pressure, which often translates into the trampling of the dunes in the areas close to the beach accesses [23,34,45]. The impacts of the front beach erosion and the damage generated over this infrastructure led to various beach nourishment projects in 1998 (737,000 m³), 2010 (102,200 m³), 2015 (105,200 m³) and 2018 (150,000 m³) [47,48].

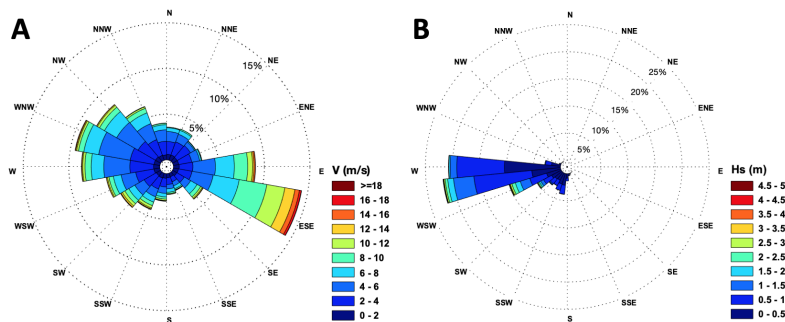


Figure 2. (A) Wind rose and (B) wave rose. The period analyzed covers 10 October 2008 to 1 February 2018. Data source: Puertos del Estado.

3. Materials and Methods

Topographic surveys were carried out at Camposoto Beach between 2008 and 2018 with a two-year gap between 2011 and 2013 (Figure 3). The evolution of the beach–dune boundary during this period was analyzed using the dune toe as a proxy. Data were collected using RTK-DGPS (a Real-Time Kinematic Differential Global Positioning System; Figure 4A) at a monthly frequency. Additionally, the dune toe data were retrieved from high-resolution images taken via UAS (Unmanned Aerial System) flights between 2017 and 2018 (Figure 4B). The UAS used was an octocopter (Atyges FV8) equipped with a 24 Mpx Sony Alpha 7 camera. Details of the flight planning and image processing can be found by consulting the work of Talavera et al. (2018) [45]. A total of 71 dune toe lines were obtained for the analyzed period, 63 from RTK-DGPS surveys and 8 from drone flight images (Figure 3). Dune positions were extracted directly from the RTK-DGPS surveys, while for the high-resolution UAS images, it was necessary to build the associated DTM and then manually digitize the dune toe. The dune toe was defined as the most seaward extension of aeolian processes and deposits [25], and it was identified in the field or extracted manually from images. In locations where the above limit was not visible, the positions of sharper slope transitions were selected [49] from both the RTK-DGPS profiles and the drone-derived DTM that was constructed.

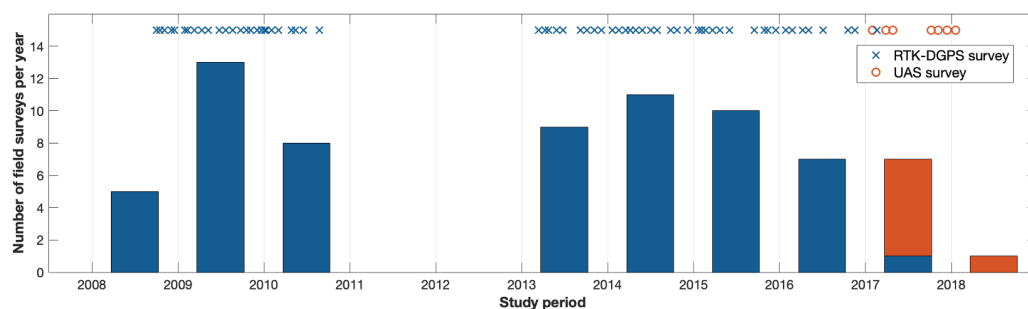


Figure 3. Distribution of the dune toe surveys carried out at Camposoto Beach over the study period differentiated by field survey type: RTK-DGPS (blue) or UAS (orange).

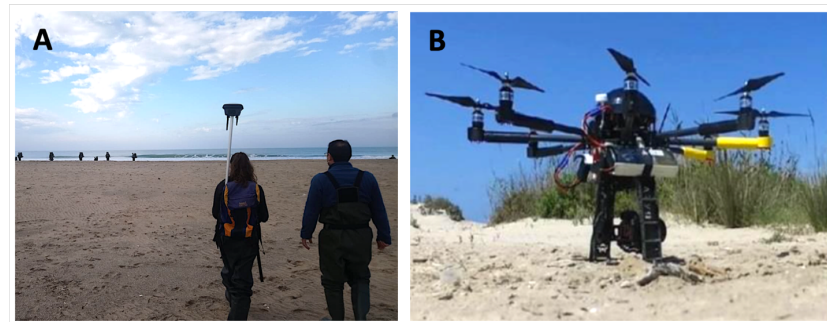


Figure 4. (A) RTK-DGPS topographic survey carried out at Camposoto Beach and the (B) octocopter used for UAS flights.

Changes in the dune toe position were assessed using a DSAS-type [50] approach. Firstly, a baseline was set parallel to the shoreline, from which 24 perpendicular profiles spaced 20 m apart were projected offshore, aiming to intersect the dune toe lines (Figure 5). The distance from the baseline of each intersection point was extracted, and the relative position of each dune toe was computed. Finally, several statistics were calculated using the equations defined by Himmelstoss et al. [50]: Net Shoreline Movement (NSM), the Shoreline Change Envelope (SCE), the End Point Rate (EPR) and the Linear Regression Rate (LRR). NSM expresses the distance (m) between the oldest and the most recent dune toes, representing the net change. SCE calculates the distance (m) between the closest point to the baseline and the farthest point (the net variability over the studied period). Finally, EPR and LRR are change rates in meters per year. The former is obtained from the eldest and most recent dune toes, while the latter is calculated with every dune toe over the period. For both rates, negative values indicate dune toe erosion and positive values indicate dune toe progradation.

Changes in the dune toe elevation (height) were also analyzed using the dune toe height evolution over the study period, as this variable could provide information about the emerged beach’s status. Then, the beach–dune relation was tested by correlating the dune toe’s mean height with the LRR of each profile.

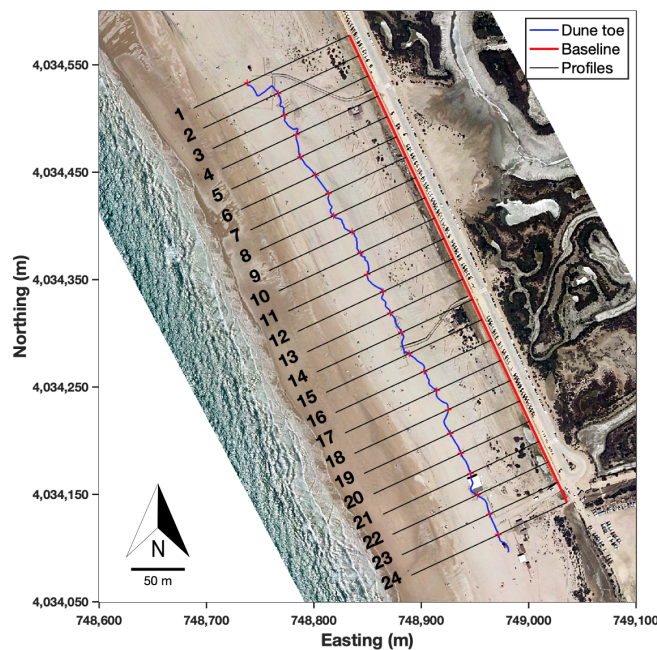


Figure 5. Methodology used to determine dune toes relative positions in reference to a baseline, from which 24 profiles were projected. Profiles 1 to 13 belong to Section 1; Profiles 15 to 24 belong to Section 2. Background image: 2018 high-resolution UAS image.

4. Results

The results were assessed after dividing the area into two sections based on the different behavior observed in the analyzed area. Section 1 includes Profiles 1 to 13, and Section 2 considers Profiles 15 to 24. Profile 14 was not considered for this analysis, as its location coincides with a wooden walkway access (see Figure 5) that generates the accumulation of sand unrelated to the natural behavior of the dune toe, thus causing data distortion.

4.1. Dune Toe Position

The analysis of the dune toe position over the study area revealed a gradual transition from a linear dune toe setting in 2008 to a more spatially variable one in 2018, as can be seen in the dune toe positions presented in Figure 6. Overall, there was a net retreat over the analyzed period, as can be observed from the initial and final position of the dune toe (the blue and red lines in Figure 6). Moreover, a different dune toe behavior can be observed between the defined sections, with a greater retreat in Section 1, where the dune toe position in 2018 presents a retreat coinciding with the development of washover fans.

Over the study period, three time intervals could be distinguished: Period 1, before the data gap (2008–2010), and Periods 2 and 3, separated by the beach nourishment project carried out in Camposoto during the spring of 2015 (Figure 7). The dune toe's relative position for the entire area of Camposoto Beach, calculated as a spatial average of all the profiles, showed a general erosion and a cyclic pattern of retreat and progradation, which was more intense in Period 1 (see Figure 7). The LRR was calculated for each time interval, at -3.56 m/year for Period 1, -2.72 m/year for Period 2, and -2.58 m/year for Period 3. For the entire study period, a mean NSM of 16.29 m was obtained, indicating a general retreat of the system, with minimum and maximum values of 0.68 m and 42.67 m, respectively. SCE (Figure 8) presented a mean value of 36.30 m, with a maximum value of 53.87 m (Profile 8) and a minimum value of 26.09 m (Profile 20). For the LRR (Figure 8), a mean retreat of 2.30 m/year was obtained. The highest erosion rate (3.61 m/year) appeared in Profile 5; meanwhile, for the rest of the beach, the retreat was less intense. The minimum LRR registered was 0.75 m/year (Profile 20). It can also be noticed in Figure 8 that high SCE values coincided with high LRR values. Furthermore, the change rate calculated using the EPR presented a mean value of -1.75 m/year.

The retreat trend observed for the entire beach and the cyclic pattern described were also present when analyzing Sections 1 and 2 separately (Figure 7). Regarding the statistics, a mean value of 20.44 m was obtained for the NSM in Section 1, versus 11.26 m in Section 2. The SCE registered a mean value of 37.77 m in Section 1, versus 35.06 m in Section 2, but the differences were greater in terms of the maximum and minimum variability, as the maximum value for Section 1 was nearly 15 m over the mean of that section (Figure 8). The mean LRR values were -2.62 m/year (Section 1) and -1.93 m/year (Section 2). In Section 1, about half of the profiles registered retreat rates of around or over 3 m/year, while in Section 2, only two profiles presented retreat rates over 2.5 m/year. The EPR presented a mean value of -2.35 m/year and -0.97 m/year for Section 1 and Section 2, respectively.

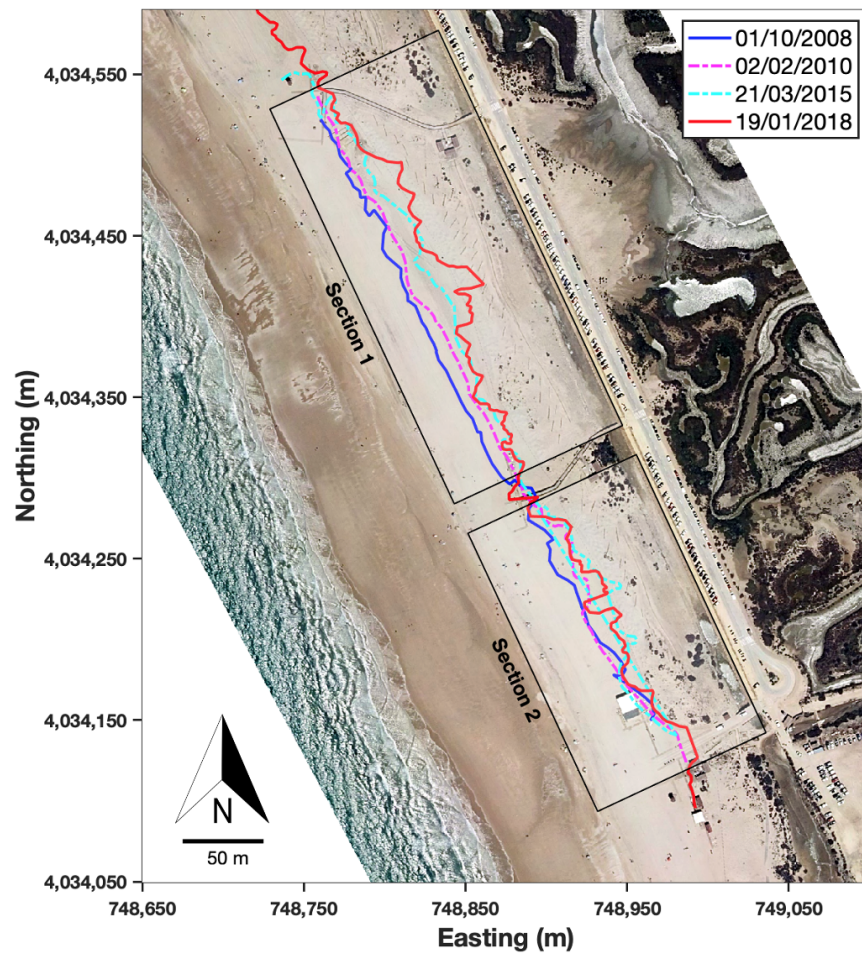


Figure 6. Dune toe projection on four different dates throughout the study area. Background image: 2018 high-resolution UAS image.

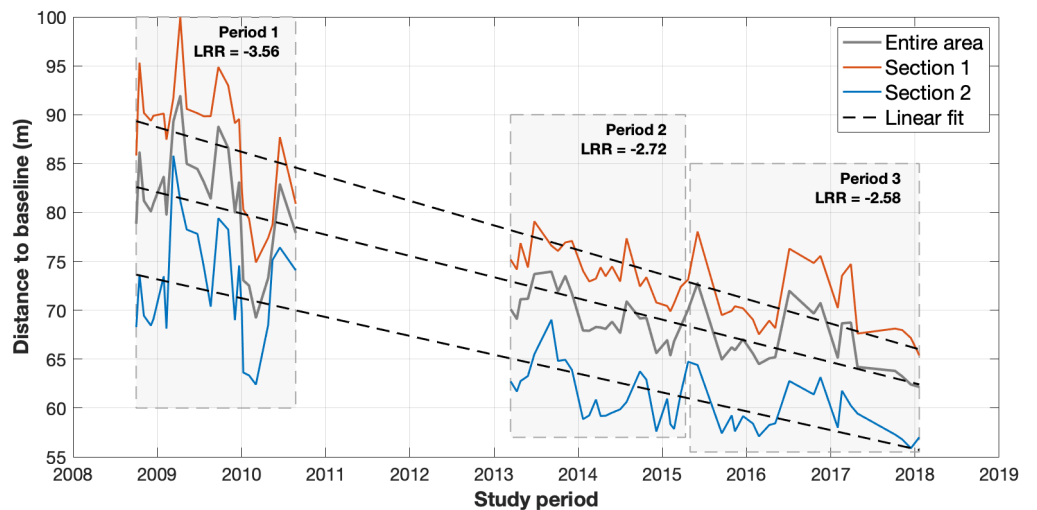


Figure 7. Evolution of the mean dune toe distance relative to the baseline over the studied period for the entire area of Camposoto Beach and for each section. The study period was divided into Period 1 (2008 to 2010), Period 2 (2013 to April 2015) and Period 3 (April 2015 to 2018). The LRR for each period (m/year) is included, referring to the entire area.

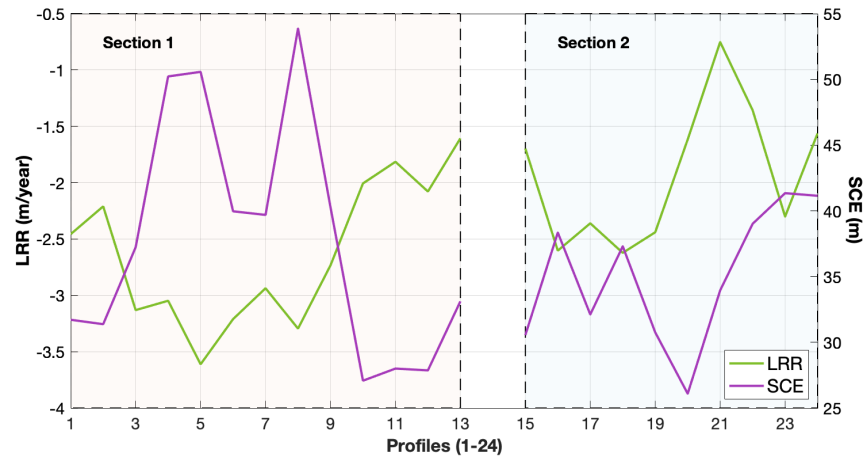


Figure 8. Linear Regression Rate (LRR) and Shoreline Change Envelope (SCE) along the 24 profiles of the study area.

4.2. Dune Toe Elevation

Using the data provided via the DGPS-RTK and the DTM obtained from the drone images, the dune toe elevation could be analyzed. This variable (Figure 9) decreased over time from a mean of 3.89 m in 2008 to 3.59 m in 2018. Once again, there was a difference between sections. The dune toe in Section 1 decreased from 3.85 m in 2008 to a mean height of 3.39 m in 2018 (nearly 0.5 m; Figure 9), whereas in Section 2, the mean height was 3.90 m in 2008, and it decreased to 3.82 m in 2018. Profile 8 exhibited the highest change in dune toe elevation, as its dune toe height decreased by more than 1 m over 10 years (from 3.84 m in 2008 to 2.64 m in 2018) (Figure 9).

In an effort to determine whether the LRR and the dune toe elevation (presented in Figures 8 and 9, respectively) were related, the relation between both variables was investigated (Figure 10) using the mean LRR and the mean dune toe elevation for each profile over the analyzed period. The linear correlation result was significant, with a value of $R_2 = 0.70$ and a p -value < 0.05 . With this result, the decrease in the dune toe elevation could be related to the beach’s progressive erosion, as the decrease in the emerged beach’s elevation increased its vulnerability to the impact of storms. Thus, it was observed that a decrease of half a meter in the elevation of the dune toe in Section 1 made the retreat of the system much greater in this area.

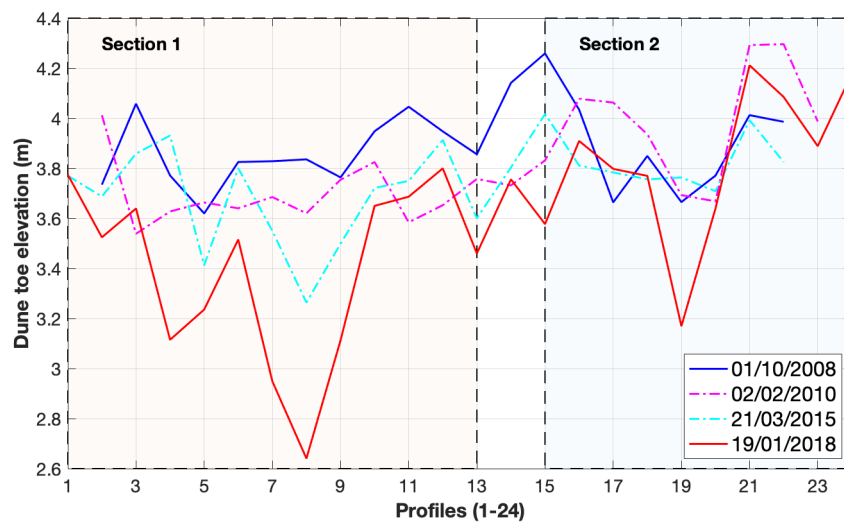


Figure 9. Evolution of the dune toe elevation along the 24 profiles. The dune toe elevation is referred to as the Hydrographic Zero.

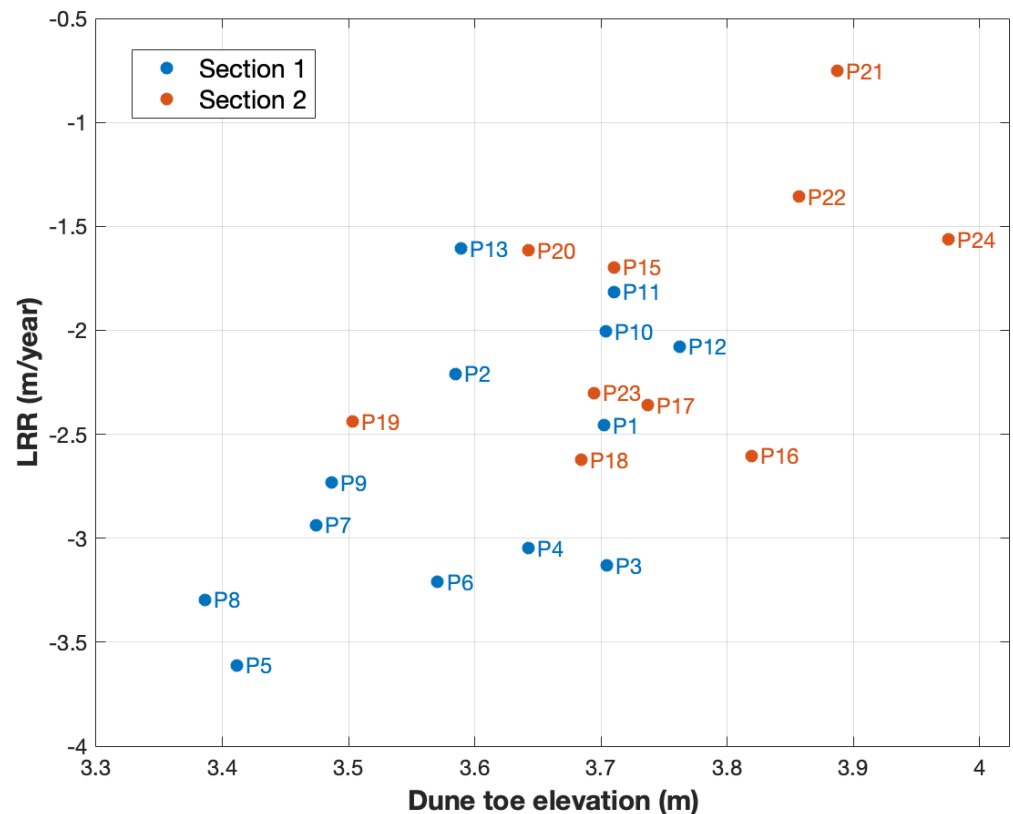


Figure 10. Relation between the medium dune toe elevation (m) for each profile (Profiles 1–24), and the LRR obtained at the same profiles.

5. Discussion

The results present the perdurance of the already identified retreating trend of the system [44,51–53], as well as an acceleration in this process for the area of Camposoto Beach, as the dune toe retreat registered in this area during the 10-year period spanning from 2008 to 2018 (-2.30 m/year) was doubled in comparison to the one presented by Del Río et al. [51] for the period from 1956 to 2008 over a wider area (an average of -0.9 m/year with maximum of 1.4 m/year). The reason for the observed differences could be methodological (different time scale resolutions) and/or physical (changes in the trend after a high-energy storm occurred in 2010, from which the beach could not fully recover). Del Río et al. [51] studied the evolution of the spit from aerial pictures and beach profiles widely distributed along the system, where it is difficult to identify short-term or seasonal changes. Puig et al. [44] identified a general trend for the same spit at different time intervals, with stages of more accelerated erosion alternating with other, more stable periods derived from natural recovery processes or artificial beach nourishment projects.

This finding is supported by the analysis carried out in the current study. In the first place, from Figure 6, an evident recession and an increase in the spatial irregularities on the dune toe can be deduced: starting in 2008 with a linear dune toe, the following dates progressively show that irregularities increased until 2018 (see Figure 6) and that the dune toe migrated landwards. These irregularities suggest foredune fragmentation (washover development and/or reactivation that was already described by Benavente et al. [39]), which is occurring simultaneously with the erosion and retreat of the dune system; these processes have increased progressively from 2008 to 2018 (Figure 7). The LRR associated with each period in Figure 7 is greater for Period 1 (-3.56 m/year). Puig et al. [44] calculated the shoreline change rate for Period 1 at -5.83 m/year, but this was estimated from only two aerial images, and this period included Storm Xynthia (February 2010). Hence, the

observed differences could be related to the spatial and temporal resolution and storm activity. Differences could also be related to the proxy used by Puig et al. [44], the high water line, which is more variable than the dune toe. Both the time scale and the proxy can influence change rate values, as observed in this comparison. After dividing the study area into Sections 1 and 2 (Figure 7), differences in their evolution can be noticed, as the retreat of the dune toe's relative position in Section 1 was more intense. This is supported by the LRR and SCE statistics (Figure 8), which made quantifying the dune toe trend and the different behaviors along the beach possible: the average erosion rate was notably higher in Section 1 (2.63 m/year) compared to Section 2 (1.93 m/year), as was the variability (SCE), though the differences in this regard are smaller (37.77 m in Section 1 versus 35.06 m in Section 2). The minimum rate observed (0.75 m/year in Profile 21) is associated with Section 2, which, as mentioned, has presented a more resilient dune toe position over the years, while the maximum retreat rates (over 3.5 m/year in Profile 5) can be associated with the washover fans that appear in Profile 9 from Section 1 (Figure 11). This would also explain the higher variability of this section, as overwash processes affect the foredune stability and contribute to its erosion.

It is likely that the dune toe retreat is related to different factors. In the first place, it is likely related to extreme events during which waves can overpass the beach and reach the foredune. This is the first step in washover fans' initiation, formation or reactivation, and it could lead to dune fragmentation, as presented in Figure 11. The washover evolution characterized by Benavente et al. [39] showed that most of the washovers observed in 2010 and 2011 had developed from the expansion of smaller ones that appeared in 2008. This was due to the higher level of energy recorded in the 2009–2010 winter season [35] and the devastating effect of the storm group recorded between 18th December and 6th January. From the analysis of washover dimensions and morphologies, and based on the proposal by Matias et al. [8], it can be concluded that the main cause of washover generation is structural erosion [39]. This, together with a lack of sediment derived in large part from heavy dam constructions in the rivers that nourish the SW coast of the Iberian Peninsula [54,55], can hinder dune recovery, and it is linked to a long-term erosion trend. Evidence of this sediment shortage includes the nourishment works performed at Camposoto over recent decades [35], as well as the outcropping of the fossil salt marsh layers of the foreshore (Figure 12), like the episodes described by Burningham [18] and Davis and Fitzgerald [19] in similar spit-barrier systems. Also, washover formation (see Figure 11) indicates a clear activation of rollover process in that area [39,46].

The observed structural erosion generates a decrease in the amount of the beach sand volume and, therefore, a decrease in its elevation with respect to sea level. The dune toe height evolution (Figure 9) showed a clear decrease (close to 0.5 m in some areas). This behavior could be attributed to the aforementioned appearance of washover fans, which erode the foredune at its lowest points [56]. The decrease in the dune toe height was again more significant in the profiles of Section 1 (Figure 9), which was probably related to the washover reactivation during storm events. This progressive decrease in the elevation of the dune toe indicates that the erosion threshold set by del Río et al. [35] decreased during the studied period, which would imply that storms with practically annual return periods or even modal waves during spring tides could be reactivating the washover fans and generating erosion at the dune toe, thereby accelerating its retreat.

The interaction between overwash processes and the dune toe position is evident when separately analyzing the two sections defined and establishing a relation between the LRR and the dune toe height (Figure 10), as the points representing Section 1 had a lower dune toe and registered higher regression; meanwhile, Section 2 (especially Profiles 20 to 24) presented a higher dune toe and remained less eroded. The dune toe retreat and lowering (Figures 8–10) denote a clear pattern of dune erosion and the net sediment loss of these geomorphological units (the beach and the dune). Although data on the dune crest height are not presented in this work, there was a clear reduction in the dune height of the sectors between 2008 and 2018, and this loss was accompanied by a reduction

in vegetation cover. The field observation during the surveys suggests that the barrier sector under study is transitioning from a vegetated island sector to an overwash sector, according to the bistability model of Durán and Moore [4], though trampling could have influenced the vegetation loss at some points before the dune area was fenced in by the local administration. Apart from that, the evolution of the dune toe (Figures 6 and 7) showed a rhythmic pattern in which recession and progradation alternated. The dune toe cyclic progradation (Figure 7) seemed ephemeral. Dunes evolve through slow changes, and progradation happens in a mid-long timescale when conditions are favorable (with not many extreme events and with adequate wind conditions) [57,58]. However, some factors can drive short-term changes in foredunes, such as wind events. When winds blow from the back of the dune ridge (offshore), airflow separation is generated in the foredune, and two areas can be distinguished: one adjacent to the foredune, where the airflow reverses its direction and blows towards the dune, and another area next to the former, where the wind keeps blowing in its initial direction [59]. Given the bimodal wind regime in Camposoto (Figure 2A), when the easterly winds blow with enough consistency, sand is remobilized and deposited on the foredune, forming sand tales (shadow dune deposits; Figure 13). The alternation of winter sea storms and summer easterly wind events that occur every year in this area could be driving the rhythmic pattern described, although this needs further research. As can be seen in Figure 7, a small degree of progradation disappears quickly without the intervention of a storm. Another factor that may have influenced the dune toe position is the beach nourishment projects carried out in the springs of 2010 and 2015, as these dates coincide with the notorious progradation of the proxy. The erosion rates identified for Periods 2 and 3 (Figure 7) are lower than the previous rates, which could be related to a greater sediment availability after the nourishment efforts. The aforementioned patterns were registered due to the high temporal resolution of the field surveys. Evidence of this includes the difference between the EPR and LRR results. The EPR presented a mean value of -1.75 m/year, whilst the mean value of the LRR was substantially greater (-2.30 m/year). This difference derives from the dune toe changes that occurred on a smaller timescale during the years of the study period that were not identified with the EPR.

Signs of barrier rollover processes have been studied at many sand and gravel spits worldwide [5,6,18,45,60–64]. These signs coincide with some of those described for Camposoto Beach (overwash processes, outcrops of peat layer patches on the intertidal area, and the narrowing of the beach due to erosion at the foreshore). However, quite often, barrier rollover processes are hindered due to anthropic infrastructure located on the back barrier, which acts as obstacles that restrict the onshore delivery of material. Some studies have evidenced how human infrastructure and interventions aiming to hinder retrograding barriers have not achieved this target and have even occasioned more erosion problems, usually at the foreshore [6,65,66]. This was also observed at Camposoto Beach, where the rollover process is blocked due to hard infrastructure placed between the dune ridge and the salt marshes. This infrastructure (wooden walkways, parking lots, a road and an artificial channel; Figure 11) is permanent, and it limits the dunes' landward migration. Taking into account the above, together with the erosion rates obtained for the dune toe, the area occupied by the dune system narrowed over the study period. As long as this infrastructure remains operative, the system will not be able to migrate landwards, thus causing dune narrowing and possibly even the drowning and/or disintegration of the barrier in this area if the sediment availability does not change. Despite managers periodically returning overwashed sediment to the dune system, additional sediment deposited past the road during high-energy events becomes disconnected.



Figure 11. Aerial picture of Camposoto Beach presenting a washover fan located in Section 1. Source: Talavera [34].



Figure 12. Outcropping of fossil salt marsh sediment on the beach of Camposoto under normal winter conditions (right) and after an extreme storm (left).

It must be mentioned that the behavior described for this study period continued afterwards. This became evident when Storm Emma affected Camposoto Beach in February–March 2018, with very high energy (the maximum significant wave height registered was 6.9 m). Its coincidence with spring tides generated an elevation of 2.1 m over the mean sea level, and the return period of the maximum significant height was estimated in 16 years [23]. Waves were able to overpass the whole dune system, and they created huge deposits of sand behind the road [46]. These dunes practically disappeared, and since 2018, no more dune toe surveys have been conducted. Beach nourishment of 150,000 m³

of sand was added to the northern part of the system, and at the same time, sand piling from the channel was used to rebuild the dunes. A detailed analysis of this event at the Camposoto barrier island can be found in Malvarez et al. [23].



Figure 13. Shadow dune deposits at Camposoto Beach.

6. Conclusions

The analysis of the dune toe evolution at Camposoto Beach showed an acceleration in the erosive trend compared with previous studies carried out at the Sancti Petri sand spit due to the action of storm events, together with a general lack of sediment budget that results in the structural erosion of the system.

This work offers a study with a higher temporal and spatial resolution, as RTK-DGPS or UAS surveys were carried out monthly when possible. This allowed for the registration of short-term changes in the beach–dune system, such as seasonal changes. Monthly fieldwork has proven to offer great information about short-term changes in the proxy, which cannot be observed with other methods, such as aerial photogrammetry. It also allows the identification of whether the changes derive from storm events or other processes that act on smaller timescales, such as wind events. In the present dune toe dataset, a rhythmic pattern alternating retreat and ephemeral progradation was noticed, possibly driven by sea storms and easterly wind events, respectively.

The mean variability increased over the years as the dune toe's relative position retreated. It was also observed that neither the retreat nor the variability occurred homogeneously along the beach. Northend profiles (Section 1) showed higher erosion rates, as well as the maximum variability, while in the southern profiles (Section 2), the dune toe remained less retreated and more stable.

The dune toe height decreased over the study period, especially in Section 1, thus contributing to the higher variability in the dune toe position of this area due to the reactivation and expansion of washover fans. These overwash processes might be influencing the dune toe erosion, as a significant relation has been established between the dune toe height and the erosion trend observed for each profile, meaning that profiles where the dune toe is lower are prone to suffering higher erosion rates and more frequent washover episodes, possibly leading to a weaker barrier system. Furthermore, given the erosion rates identified in this work, future interference with the infrastructure present in the area is probable.

Author Contributions: Conceptualization, T.A.P., J.B. and C.M.; fieldwork, T.A.P., M.P., J.M., C.M., L.T. and J.B.; data curation, C.M., T.A.P., J.M., M.P. and L.T.; graphics, C.M., J.M. and T.A.P.; writing—original draft preparation, C.M. and T.A.P.; writing—review and editing, C.M., J.B., T.A.P., J.M., M.P. and L.T.; supervision, J.B. and T.A.P.; project administration, T.A.P. and J.B.; funding acquisition, T.A.P. and J.B. All authors have read and agreed to the published version of the manuscript.

Funding: This research was funded by the Regional Andalucian government and the European Union under the CRUNCH project (FEDER-UCA18-107062) and the Spanish Ministry of Science and Innovation under the CRISIS project (PID2019-109143RB-I00).

Data Availability Statement: Data can be available on reasonable request from the corresponding author.

Acknowledgments: This work is a contribution of the Andalusian PAI research group RNM-328. The authors are grateful for the collaboration and support of all students, technical staff and researchers who contributed to the project's fieldwork. The orthophotos used in this work were supplied by the National Geographical Institute of Spain (IGN), and the wave data were made available from the Puertos del Estado, while the tidal data were made available by the Spanish Institute of Oceanography (IEO). Juan Montes holds a Margarita Salas postdoctoral fellowship from the University of Cadiz, and Lara Talavera holds a postdoctoral grant modality, 'María Zambrano', both for the Requalification of Spanish University System 2023–2024, funded by the European Union-NextGenerationEU.

Conflicts of Interest: The authors declare no conflicts of interest.

References

1. Stutz, M. L.; Pilkey, O.H. Global Distribution and Geomorphology of Fetch-Limited Barrier Islands. *J. Coast. Res.* **2001**, *25*, 819–837.
2. Moore, L.J.; List, J.H.; Williams, S.J.; Stolper, D. Complexities in barrier island response to sea level rise: Insights from numerical model experiments, North Carolina Outer Banks. *J. Geophys. Res.* **2010**, *115*, F03004. [[CrossRef](#)]
3. Delgado-Fernandez, I.; Davidson-Arnott, R. Meso-scale aeolian sediment input to coastal dunes: The nature of aeolian transport events. *Geomorphology* **2011**, *126*, 217–232. [[CrossRef](#)]
4. Durán Vinent, O.; Moore, L.J. Barrier island bistability induced by biophysical interactions. *Nat. Clim. Chang.* **2015**, *5*, 158–162. [[CrossRef](#)]
5. Devoy, R.J.N. *The Development and Management of the Dingle Bay Spit-Barrier of Southwest Ireland*; Springer International Publishing: Cham, Switzerland, 2015; pp. 139–180. [[CrossRef](#)]
6. Stéphan, P.; Suanez, S.; Fichaut, B. *Long-, Mid- and Short-Term Evolution of Coastal Gravel Spits of Brittany, France*; Springer International Publishing: Cham, Switzerland, 2015; pp. 275–288. [[CrossRef](#)]
7. Raff, J.L.; Shawler, J.L.; Ciarletta, D.J.; Hein, E.A.; Lorenzo-Trueba, J.; Hein, C.J. Insights into barrier-island stability derived from transgressive/regressive state changes of Parramore Island, Virginia. *Mar. Geol.* **2018**, *403*, 1–19. [[CrossRef](#)]
8. Matias, A.; Ferreira, O.; Vila-Concejo, A.; Garcia, T.; Dias, J.A. Classification of washover dynamics in barrier islands. *Geomorphology* **2008**, *97*, 655–674. [[CrossRef](#)]
9. D'Alessandro, F.; Tomasicchio, G.R. Wave–dune interaction and beach resilience in large-scale physical model tests. *Coast. Eng.* **2016**, *116*, 15–25. [[CrossRef](#)]
10. Lorenzo-Trueba, J.; Ashton, A.D. Rollover, drowning, and discontinuous retreat: Distinct modes of barrier response to sea-level rise arising from a simple morphodynamic model. *J. Geophys. Res. Earth Surf.* **2014**, *119*, 2013JF002941. [[CrossRef](#)]
11. Reeves, I.R.; Moore, L.J.; Murray, A.B.; Anarde, K.A.; Goldstein, E.B. Dune Dynamics Drive Discontinuous Barrier Retreat. *Geophys. Res. Lett.* **2021**, *48*, e2021GL092958. [[CrossRef](#)]
12. Kombiadou, K.; Matias, A.; Costas, S.; Rita Carrasco, A.; Plomaritis, T.A.; Ferreira, Ó. Barrier island resilience assessment: Applying the ecological principles to geomorphological data. *CATENA* **2020**, *194*, 104755. [[CrossRef](#)]
13. Sherman, D.J.; Bauer, B.O. Dynamics of beach-dune systems. *Prog. Phys. Geogr. Earth Environ.* **1993**, *17*, 413–447. [[CrossRef](#)]
14. Thom, B.G.; Hall, W. Behavior of beach profiles during accretion and erosion dominated periods. *Earth Surf. Process. Landforms* **1991**, *16*, 113–127. [[CrossRef](#)]
15. Takeda, I.; Sunamura, T. Beach changes by storm waves. In *Coastal Engineering Proceedings*; American Society of Civil Engineers: Reston, VA, USA, 1986; p. 118.
16. García-Mora, M.R.; Gallego-Fernández, J.B.; Williams, A.T.; García-Novo, F. A coastal dune vulnerability classification. A case study of the SW Iberian Peninsula. *J. Coast. Res.* **2001**, *17*, 802–811.
17. Sanjaume, E.; Gracia, F.J.; Flor, G.S. Introducción a la geomorfología de sistemas dunares. In *Las Dunas en España*; Sociedad española de Geomorfología: Madrid, Spain, 2011; pp. 13–63.
18. Burningham, H. Gravel Spit-Inlet Dynamics: Orford Spit, UK. In *Sand and Gravel Spits*; Randazzo, G., Jackson, D.W., Cooper, J.A.G., Eds.; Springer International Publishing: Cham, Switzerland, 2015; Volume 12, pp. 51–65. [[CrossRef](#)]
19. Davis, R.A.; Fitzgerald, D.M. *Beaches and Coasts*, 2nd ed.; John Wiley & Sons: Hoboken, NJ, USA, 2004.
20. Kombiadou, K.; Costas, S.; Carrasco, A.R.; Plomaritis, T.A.; Ferreira, O.; Matias, A. Bridging the gap between resilience and geomorphology of complex coastal systems. *Earth-Sci. Rev.* **2019**, *198*, 102934. [[CrossRef](#)]

21. Cooper, J.A.G.; Pile, J. The adaptation-resistance spectrum: A classification of contemporary adaptation approaches to climate-related coastal change. *Ocean. Coast. Manag.* **2014**, *94*, 90–98. [[CrossRef](#)]
22. Hanley, M.E.; Hoggart, S.P.G.; Simmonds, D.J.; Bichot, A.; Colangelo, M.A.; Bozzeda, F.; Heurtefeux, H.; Ondiviela, B.; Ostrowski, R.; Recio, M. Shifting sands? Coastal protection by sand banks, beaches and dunes. *Coast. Eng.* **2014**, *87*, 136–146. [[CrossRef](#)]
23. Malvárez, G.; Ferreira, O.; Navas, F.; Cooper, J.A.G.; Gracia-Prieto, F.J.; Talavera, L. Storm impacts on a coupled human-natural coastal system: Resilience of developed coasts. *Sci. Total. Environ.* **2021**, *768*, 144987. [[CrossRef](#)]
24. Roig-Munar, F.X.; Prieto, J.A.M.; Pintó, J.; Rodríguez-Perea, A.; Gelabert, B. Coastal management in the Balearic Islands. In *The Spanish Coastal Systems*; Springer: Berlin/Heidelberg, Germany, 2019; pp. 765–787.
25. Smith, A.; Houser, C.; Lehner, J.; George, E.; Lunardi, B. Crowd-sourced identification of the beach-dune interface. *Geomorphology* **2020**, *367*, 107321. [[CrossRef](#)]
26. Biauxque, M.; Senechal, N. Seasonal morphological response of an open sandy beach to winter wave conditions: The example of Biscarrosse beach, SW France. *Geomorphology* **2019**, *332*, 157–169. [[CrossRef](#)]
27. Castelle, B.; Marieu, V.; Bujan, S.; Splinter, K.D.; Robinet, A.; Senechal, N.; Ferreira, S. On The Impact of a Series of Severe Storms on a Double-Barred Sandy Coast: Dune Erosion and Megacups Embayments. In *The Proceedings of the Coastal Sediments 2015*; World Scientific: Singapore, 2015.
28. Castelle, B.; Bujan, S.; Ferreira, S.; Dodet, G. Foredune morphological changes and beach recovery from the extreme 2013/2014 winter at a high-energy sandy coast. *Mar. Geol.* **2017**, *385*, 41–55. [[CrossRef](#)]
29. del Río, L.; Gracia, F.J. Error determination in the photogrammetric assessment of shoreline changes. *Nat. Hazards* **2013**, *65*, 2385–2397. [[CrossRef](#)]
30. Lerma, A.N.; Ayache, B.; Ulvoas, B.; Paris, F.; Bernon, N.; Bulteau, T.; Mallet, C. Pluriannual beach-dune evolutions at regional scale: Erosion and recovery sequences analysis along the aquitaine coast based on airborne LiDAR data. *Cont. Shelf Res.* **2019**, *189*, 103974. [[CrossRef](#)]
31. Lerma, A.N.; Castelle, B.; Marieu, V.; Robinet, A.; Bulteau, T.; Bernon, N.; Mallet, C. Decadal beach-dune profile monitoring along a 230-km high-energy sandy coast: Aquitaine, southwest France. *Appl. Geogr.* **2022**, *139*, 102645. [[CrossRef](#)]
32. Mélanie, B.; Senechal, N.; Barre, A.; Laigre, T. High frequency monitoring of the shoreline/barline evolution of an open sandy beach, the example of Biscarrosse Beach (France). *Proc. Coast. Dyn.* **2017**, 567–574.
33. Vandenhove, M.; Castelle, B.; Lerma, A.N.; Marieu, V.; Mallet, C.; Mazeiraud, V. Multidecadal shoreline variability linked with estuarine sandbank welding: The North Medoc Coast, Southwest France. In *Coastal Sediments 2023: The Proceedings of the Coastal Sediments 2023*; World Scientific: Singapore, 2023; pp. 1452–1457.
34. Talavera, L. UAS-Based Monitoring of Sandy Coasts in the Bay of Cadiz (SW Spain). Ph.D. Thesis, Universidad de Cádiz, Cádiz, Spain, 2019.
35. Del Rio, L.; Plomaritis, T.A.; Benavente, J.; Valladares, M.; Ribera, P. Establishing storm thresholds for the Spanish Gulf of Cadiz coast. *Geomorphology* **2012**, *143–144*, 13–23. [[CrossRef](#)]
36. Bellido, C.; Anfuso, G.; Plomaritis, T.A.; Rangel-Buitrago, N. Morphodynamic behaviour, disturbance depth and longshore transport at Camposoto Beach (Cadiz, SW Spain). *J. Coast. Res.* **2011**, *SI 64*, 35–39.
37. Plomaritis, T.A.; Anfuso, G.; Benavente, J.; Del Río, L. Storm impact and recovery patterns in natural and urbanised beaches in Cádiz (SW Spain). In *Proceedings of the EGU General Assembly Conference Abstracts*, Vienna, Austria, 19–24 April 2009; p. 1409.
38. IHN. *Anuario de Mareas 2023*; Ministerio de Defensa: Madrid, Spain, 2023.
39. Benavente, J.; Río, L.d.; Plomaritis, T.A.; Menapace, W. Impact of coastal storms in a sandy barrier (Sancti Petri, Spain). *J. Coast. Res.* **2013**, *65*, 666–671. [[CrossRef](#)]
40. Rangel-Buitrago, N.; Anfuso, G. Winter wave climate, storms and regional cycles: The SW Spanish Atlantic coast. *Int. J. Climatol.* **2013**, *33*, 2142–2156. [[CrossRef](#)]
41. Plomaritis, T.A.; Benavente, J.; Laiz, I.; Del Río, L. Variability in storm climate along the Gulf of Cadiz: The role of large scale atmospheric forcing and implications to coastal hazards. *Clim. Dyn.* **2015**, *45*, 2499–2514. [[CrossRef](#)]
42. Del Río, L.; Benavente, J.; Gracia, F.; Anfuso, G.; Aranda, M.; Montes, J.B.; Puig, M.; Talavera, L.; Plomaritis, T.A. *Beaches of Cadiz*; Springer International Publishing: Cham, Switzerland, 2019; pp. 311–334. [[CrossRef](#)]
43. Fernández-Montblanc, T.; Del Río, L.; Izquierdo, A.; Gracia, F.J.; Bethencourt, M.; Benavente, J. Shipwrecks and man-made coastal structures as indicators of historical shoreline position. An interdisciplinary study in the Sancti Petri sand spit (Bay of Cádiz, SW Spain). *Mar. Geol.* **2018**, *395*, 152–167. [[CrossRef](#)]
44. Puig, M.; del Río, L.; Plomaritis, T.A.; Benavente, J. Contribution of storms to shoreline changes in mesotidal dissipative beaches: Case study in the Gulf of Cádiz (SW Spain). *Nat. Hazards Earth Syst. Sci.* **2016**, *16*, 2543–2557. [[CrossRef](#)]
45. Talavera, L.; Del Río, L.; Benavente, J.; Barbero, L.; López-Ramírez, J.A. UAS as tools for rapid detection of storm-induced morphodynamic changes at Camposoto beach, SW Spain. *Int. J. Remote. Sens.* **2018**, *39*, 5550–5567. [[CrossRef](#)]
46. Talavera, L.; del Río, L.; Benavente, J. UAS-based High-resolution Record of the Response of a Seminatual Sandy Spit to a Severe Storm. *J. Coast. Res.* **2020**, *95*, 679–683. [[CrossRef](#)]
47. Román-Sierra, J.; Muñoz-Perez, J.J.; Navarro-Pons, M. Beach nourishment effects on sand porosity variability. *Coast. Eng.* **2014**, *83*, 221–232. [[CrossRef](#)]

48. Santos-Vendoiro, J.J.; Muñoz-Perez, J.J.; Lopez-García, P.; Jodar, J.M.; Mera, J.; Contreras, A.; Contreras, F.; Jigena, B. Evolution of Sediment Parameters after a Beach Nourishment. *Land* **2021**, *10*, 914. [[CrossRef](#)]
49. Stockdon, H.F.; Sallenger, A.H., Jr.; Holman, R.A.; Howd, P.A. A simple model for the spatially-variable coastal response to hurricanes. *Mar. Geol.* **2007**, *238*, 1–20. [[CrossRef](#)]
50. Himmelstoss, E.A.; Henderson, R.E.; Kratzmann, M.G.; Farris, A.S. *Digital Shoreline Analysis System (DSAS)*; U.S. Geological Survey: Woods Hole, MA, USA, 2018.
51. Del Río, L.; Gracia, F.J.; Benavente, J. Shoreline change patterns in sandy coasts. A case study in SW Spain. *Geomorphology* **2013**, *196*, 252–266. [[CrossRef](#)]
52. Puig, M.; del Río, L.; Plomaritis, T.A.; Benavente, J. Influence of storms on coastal retreat in SW Spain. *J. Coast. Res.* **2014**, *70*, 193–198. [[CrossRef](#)]
53. Puig, M.; González, J.B.; Plomaritis, T.A.; del Río Rodríguez, L. Estudio de los eventos de recuperación en dos playas de la Bahía de Cádiz (Playa de La Victoria y Playa de Camposoto). *Geotemas* **2015**, *15*, 69–72.
54. Polo, M.J.; Rovira, A.; García-Contreras, D.; Contreras, E.; Millares, A.; Aguilar, C.; Losada, M.A. Reservoir impacts downstream in highly regulated river basins: The Ebro delta and the Guadalquivir estuary in Spain. *Proc. Int. Assoc. Hydrol. Sci.* **2016**, *373*, 45–49. [[CrossRef](#)]
55. Walling, D.E. The role of dams in the global sediment budget. *IAHS-AISH Publ.* **2012**, *356*, 3–11.
56. Reyes, J.; Benavente, J.; Gracia, F.J.; López-Aguayo, F. Efectos de los temporales sobre las playas de la Bahía de Cádiz. In *IV Reunión de Geomorfología*; Sociedad Española de Geomorfología: A Coruña, Spain, 1996.
57. Farrell, E.J.; Delgado Fernandez, I.; Smyth, T.; Li, B.; Swann, C. Contemporary research in coastal dunes and aeolian processes. *Earth Surf. Process. Landforms* **2024**, *49*, 108–116. [[CrossRef](#)]
58. Walker, I.J.; Davidson-Arnott, R.G.; Bauer, B.O.; Hesp, P.A.; Delgado-Fernandez, I.; Ollerhead, J.; Smyth, T.A. Scale-dependent perspectives on the geomorphology and evolution of beach-dune systems. *Earth-Sci. Rev.* **2017**, *171*, 220–253. [[CrossRef](#)]
59. Delgado-Fernandez, I.; Jackson, D.W.T.; Cooper, J.A.G.; Baas, A.C.W.; Beyers, J.H.M.; Lynch, K. Field characterization of three-dimensional lee-side airflow patterns under offshore winds at a beach-dune system. *J. Geophys. Res. Earth Surf.* **2013**, *118*, 706–721. [[CrossRef](#)]
60. Bujalesky, G.G.; Gonzalez Bonorino, G. El Paramo Transgressive Gravel Spit, Tierra del Fuego, Argentina. In *Sand and Gravel Spits*; Randazzo, G., Jackson, D.W., Cooper, J.A.G., Eds.; Coastal Research Library; Springer International Publishing: Cham, Switzerland, 2015; pp. 37–50. [[CrossRef](#)]
61. Carmona, P.; Ruiz, J.M.; Pérez-Cueva, A.; Acosta, M.L. Accelerated transgressive processes in a Mediterranean coastal barrier: Subsidence, anthropic action and geomorphological changes since the Little Ice Age. *Quat. Int.* **2020**, *554*, 150–163. [[CrossRef](#)]
62. Regnaud, H.; Costa, S.; Musereau, J. Spits on the French Atlantic and Channel Coasts: Morphological Behaviour and Present Management Policies. In *Sand and Gravel Spits*; Randazzo, G., Jackson, D.W., Cooper, J.A.G., Eds.; Springer International Publishing: Cham, Switzerland, 2015; Volume 12, pp. 247–258. [[CrossRef](#)]
63. Tillmann, T. Geomorphology and Internal Sedimentary Structure of a Landward Migrating Barrier Spit (Southern Sylt/German Bight): Insights from GPR Surveys. In *Sand and Gravel Spits*; Randazzo, G., Jackson, D.W., Cooper, J.A.G., Eds.; Springer International Publishing: Cham, Switzerland, 2015; Volume 12, pp. 307–325. [[CrossRef](#)]
64. Vespremeanu-Stroe, A.; Preoteasa, L. Morphology and the Cyclic Evolution of Danube Delta Spits. In *Sand and Gravel Spits*; Randazzo, G., Jackson, D.W., Cooper, J.A.G., Eds.; Springer International Publishing: Cham, Switzerland, 2015; Volume 12, pp. 327–339. [[CrossRef](#)]
65. Bellis JR, V.J.; O'Connor, M.; Riggs, S.R. *Estuarine Shoreline Erosion in the Albemarle-Pamlico Region of North Carolina*; UNC Sea Grant: Raleigh, NC, USA, 1975.
66. Randazzo, G.; Jackson, D.W.; Cooper, J.A.G. (Eds.) *Sand and Gravel Spits*; Coastal Research Library; Springer International Publishing: Cham, Switzerland, 2015; Volume 12. [[CrossRef](#)]

Disclaimer/Publisher's Note: The statements, opinions and data contained in all publications are solely those of the individual author(s) and contributor(s) and not of MDPI and/or the editor(s). MDPI and/or the editor(s) disclaim responsibility for any injury to people or property resulting from any ideas, methods, instructions or products referred to in the content.